HIGH SCHOOL EDITION
Journal of Student Research
Volume 14 Issue 1 (2025)

Toxicity and Bioaccumulation of Surface Modified Graphene Quantum Dots in Zebrafish Embryos and Larvae

Hanqiao Li[1], Bo Li[#], Haotian Chen[#] and Wenhong Fan[#]

[1]The Experimental High School Attached to Beijing Normal University, China
[#]Advisor

ABSTRACT

Surface modified Graphene Quantum Dots (GQDs) are an important class of carbon materials widely adopted in fields such as optoelectronics and medicine. However, current research on the potential threat of GQDs on humans and the environment is limited and often lacks comparisons of the biological accumulation and toxicity effects caused by different surface functional group modifications. Therefore, this study compared the toxicity of growth and development, and biological accumulation of amino-functionalized GQDs and carboxyl-functionalized GQDs in zebrafish. The results showed that both amino-functionalized and carboxyl-functionalized GQDs at concentrations of 0.5 $mg \cdot L^{-1}$ and 5 $mg \cdot L^{-1}$ significantly inhibited the spontaneous movement of zebrafish, induced pericardial edema and yolk sac edema, and stimulated approximately 50% of the zebrafish to hatch earlier. The type of material and exposure concentration had no significant effect on the zebrafish's heart rate or body length. Additionally, this study used molecular fluorescence spectroscopy to measure the biological accumulation of the two materials in zebrafish after 4 days of exposure. The results indicated that carboxyl-functionalized GQDs had higher accumulation concentration and mass percentage in zebrafish than amino-functionalized GQDs, with a total accumulation of approximately 5.6 μg. Overall, carboxyl-functionalized GQDs exhibited stronger biological accumulation and toxicity effects than amino-functionalized GQDs. This study systematically reveals the differences in biological accumulation and toxicity effects of GQDs with different surface functional groups, providing evidence and a theoretical basis for assessing the ecological risks of GQDs with various surface modifications.

Introduction

Carbon nanomaterials (CNMs) are materials that have a one-dimensional scale of less than 100 nm in three-dimensional space and exhibit a high degree of uniformity, mainly covering materials such as Fullerene, Graphene, and Carbon nanotubes. Because of their high electrical and thermal conductivity and mechanical strength, stable chemical properties, and excellent optical properties, they have been widely used as a novel material for energy and environmental science, as well as health care and medical science[1,2]. In biomedical science, carbon nanomaterials such as graphene are widely used in biosensors due to their high sensitivity, accuracy, and detection speed[3]. Carbon nanomaterials including carbon nanotubes become increasingly important for medical purposes, such as bone tissue engineering, nerve repairing, and as drug carriers[4,5].

Graphene, as a type of carbon nanomaterial, possesses immense potential in materials science, electronics, and energy storage, due to its high specific surface area, ideal electrical and thermal conductivity, strong mechanical properties, and good biocompatibility[6,7]. However, as the range of applications expands, the negative impacts of carbon nanomaterials, particularly graphene, on the environment and biological health have attracted widespread attention[8-12]. Toxicological studies indicate that carbon nanomaterials, such as fullerenes (nC60 and C60 derivatives),

upon entering cells, can induce oxidative stress, leading to the generation of reactive oxygen species (ROS) and other free radicals within biological systems, which in turn cause DNA damage and cell death[13,14].

Graphene quantum dots (GQDs) are nanoscale derivatives synthesized from graphene sheets. Due to their strong fluorescence in aqueous solutions and small sizes, they are widely adopted for optoelectronic sensors, bio-optical imaging, and drug delivery[15,16]. To further optimize the optoelectronic properties and biomedical applications of GQDs, research has focused on surface modification by introducing various surface functional groups, resulting in GQDs with different surface structures, such as carboxyl-functionalized graphene quantum dots (CGQDs) and amino-functionalized graphene quantum dots (AGQDs). Among these, GOQDs, CGQDs, and AGQDs have been widely applied in areas like fluorescent bioimaging and biosensing[17]. For instance, a study by Rosddi indicates that a novel nanocomposite film prepared by modifying cationic nano-crystalline cellulose (NCC) CGQDs exhibits superior performance in glucose sensing[18]. The structure of GQDs and their applications are shown in Figure 1.

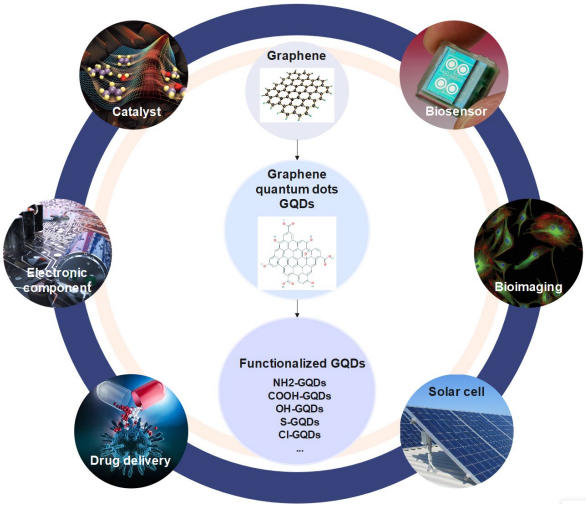

Figure 1. Graphene quantum dots and its application

With the increasing application of GQDs in recent years, their biological toxicity has also attracted considerable attention. While GQDs are generally considered to have high biocompatibility as drug carriers[19-21], several studies still indicate that they pose certain toxicological risks to living organisms, including inducing oxidative stress and genetic interference[22]. Research on the toxicological effects of GQDs suggests that their toxicity is influenced by particle size, type, and surface modifications. For instance[23], the proliferation of human A549 lung carcinoma cells and neural glioma C6 cells decreased significantly with DMF (Dimethylformamide) functionalized GQDs at 200 μg/mL. Similarly, research by Deng, S. et al. indicated that nitrogen-doped GQDs (N-GQDs) exhibit strong fluorescence permeability and tissue-specific bioaccumulation effects, and can strongly interfere with redox-sensitive systems in zebrafish by selectively inhibiting endogenous antioxidant enzyme activities[24]. Furthermore, a study by Ming Li et al. found that even at relatively low exposure concentrations (25 μg/mL), hydroxylated graphene quantum dots (HO-GQDs) exhibited high toxicity to human oral epithelial cells, causing DNA damage and cell cycle arrest, inhibiting DNA repair, disrupting microtubule structure, and hindering cell regeneration[25].

Compared with other carbon nanomaterials, the eco-toxicological studies on graphene quantum dots are scarce, and only cover GOQDs[26,27]. The materials such as GOQDs, CGQDs, and AGQDs have been widely used, but due to the different surface functional group modifications, they have different chemical properties and toxicological effects. However, the types of modifications of GQDs materials studied so far are relatively limited, so the toxicity studies of GQDs with different surface modifications need to be enriched. Specific questions include the differences in biological developmental toxicity and ecological health risks of GQDs with different surface functional groups, and

whether the toxic effects are significantly exacerbated at different concentrations. In this study, AGQDs and CGQDs were used with the aim of investigating their ecotoxicological effects at different concentrations, which is important for the application of GQDs and risk assessment in aquatic ecosystems.

Zebrafish (Danio rerio) is an important model organism in environmental toxicology, ecotoxicology, and pharmacotoxicology, with up to 87% homology to the human genome, and with physiological structures and functions similar to those of mammals, so its test results are mostly applicable to humans. In addition, since the 1970s and 1980s, researchers from many countries around the world have utilized zebrafish to carry out acute and chronic exposure toxicity experiments of chemical substances, and its application as a test organism is widespread and mature[28,29].

Aiming to fill the research gap about the toxicological effects of these two materials and to establish the correlation between the structure of GQDs surface group modification and the toxicity strength, this study selected amino- and carboxyl-modified AGQDs and CGQDs as the representative materials of graphene quantum dots. In addition, the toxicity and bioaccumulation effects at different concentrations on the growth and development of zebrafish embryos and juveniles were compared, and the toxicity differences were analyzed. This study provides a comprehensive analysis of the variations in biological accumulation and toxicity effects of GQDs with different surface functional groups, providing both data and a theoretical framework for evaluating the ecological risks associated with functionalized GQDs, to offer insights for future surface modifications to reduce toxicity.

Methods

Materials and Apparatus

The apparatus are listed here: Hitachi F-7000 Steady-State Fluorescence Spectrometer (Shanghai Ruidi Electronic Technology Co., Ltd.); Zeiss Axio Scope.A1 Research-grade Upright Microscope (Tianjin Sales Automation Technology Co., Ltd.); Upright Fluorescence Microscope (ISH300 3.0MP) (Shanghai Cewei Optoelectronics Co., Ltd.); Desktop Centrifuge (Shanghai Lixinjian Centrifuge Co., Ltd.); 24-Well Cell Culture Plates (Suzhou Saipu Biotechnology Co., Ltd.)

AGQDs N100 were purchased from Jiangsu Xianfeng Nanomaterials Technology Co., Ltd. CGQDs were purchased from Jiangsu Xianfeng Nanomaterials Technology Co., Ltd. Their properties are shown in Table 1.

Table 1. The basic properties of two graphene quantum dots (GQDs)

	AGQD	CGQD
Material Condition	Aqueous dispersion (1000 mg·L^{-1})	Aqueous dispersion (1000 mg·L^{-1})
Particle Size	3.5-5.0 nm	<10 nm
Excitation Wavelength	379±2 nm	395±2 nm
Emission Wavelength	480±2 nm	487±2 nm

The zebrafish breeders (wild-type AB, purchased from the Institute of Hydrobiology, Chinese Academy of Sciences) were housed in an automated flow-through breeding system. There were approximately 30 pairs of breeding zebrafish, with a male-to-female ratio of 1:3. The embryos and larvae used in the experiment were a mix from different breeding pairs. The flow-through system included a filter (to capture large particles in the water), a biological filter (providing a growth substrate for nitrogen-fixing bacteria), and a UV light (for disinfection). The water temperature

was maintained at 27±0.5°C, pH at 7.2±0.5, conductivity at 500 μS/cm, and the light cycle was 14:10 hours (day/night). The breeders were fed twice daily with brine shrimp (Artemia nauplii).

To prepare the embryo-larvae nutrient solution, the embryos and larvae were cultured and exposed in Hanks buffer. The Hanks buffer was prepared according to ISO-7346-3[30], containing 0.074 mmol K^+, 0.5 mmol/L Mg^{2+}, 0.75 mmol/L Na^+, and 2 mmol/L Ca^{2+}. The pH of the Hanks buffer was adjusted to around 7.2, filtered for sterilization, and then aliquoted into 500 mL sterilized glass bottles, stored at 4°C.

At the start of the zebrafish light cycle, the partition in the breeding box was removed, and the male and female zebrafish were allowed to naturally mate for 1 hour. The fertilized eggs were then collected in a petri dish. Using a plastic pipette, impurities, and excess water were removed from the petri dish, and the fresh nutrient solution was added for washing. This cleaning procedure was repeated 2-3 times, after which the eggs were placed in the incubator and cultured until 3 hours post-fertilization (hpf) for exposure experiments.

The Exposure of AGQDs and CGQDs to Zebrafish Embryos

The experiment procedure of AGQDs and CGQDs exposure and measure of bioaccumulation are figured in Fig.2.

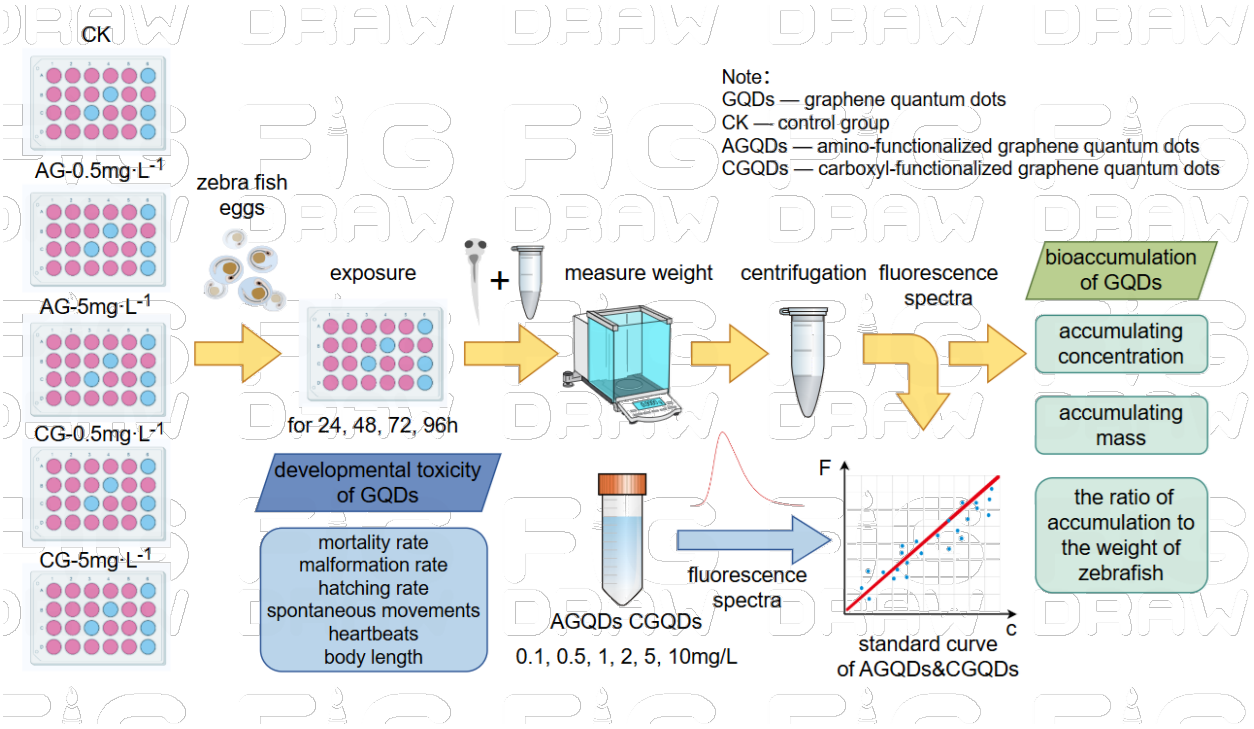

Figure 2. Flow chart of the experiment

300 μL of 1000 mg·L^{-1} AGQDs was taken and diluted with nutrient solution to a final volume of 300 mL, resulting in a 1 mg·L^{-1} AGQDs exposure solution. Similarly, 3000 μL of 1000 mg·L^{-1} AGQDs was diluted with nutrient solution to 300 mL, resulting in a 10 mg·L^{-1} AGQDs exposure solution. The preparation method for 1 mg·L^{-1} and 10 mg·L^{-1} CGQDs exposure solutions was the same as the above steps.

Dead fertilized eggs that had solidified were removed, and 1 mL of nutrient solution containing a single fertilized egg was added to each well of a 24-well plate. Three 24-well plates were grouped together, with 1 mL of nutrient solution, 1 mg·L^{-1} AGQDs exposure solution, 10 mg·L^{-1} AGQDs exposure solution, and CGQDs exposure solution added to each well within each group. The zebrafish embryos were exposed to nutrient solution (blank control

group, CK) and AGQDs and CGQDs exposure solutions at concentrations of 0.5 and 5 mg·L⁻¹ (AG-0.5, AG-5, CG-0.5, CG-5) for 96 hours. Three parallel experimental groups (three 24-well plates) were set for each group, with a total of 72 embryos and larvae observed per group. The exposure experiment was conducted in an incubator at 27 ± 0.5°C with a 14:10 hour light/dark cycle.

The 5 experimental groups of zebrafish were placed in 15 24-well plates for a 96-hour exposure experiment. The development of the zebrafish embryos and larvae was observed and recorded using an upright fluorescence microscope (ISH300 3.0MP).

The Observation of Developmental Toxicity of GQDs to Zebrafish

After 24 hours of exposure, the embryo mortality rate was recorded, and 5 embryos were randomly selected from each well plate to record the number of voluntary movements within 20 seconds. After 48 hours, the mortality rate, malformation rate, and hatchability were recorded. Additionally, 5 embryos (larvae) were randomly selected from each well plate to record the number of heartbeats within 20 seconds. The observations at 72 hpf (hours post-fertilization) were the same as at 48 hpf. At 96 hpf, the recordings were the same as at 48 hpf, with the addition of measuring the body length of 5 larvae randomly selected from each well plate. The criteria for determining death included: embryos that had solidified and turned white, showing no movement for an extended period, no heartbeat, and no blood flow. The criteria for determining malformations included: shortened or curved tails, yolk sac and pericardial edema and hyperemia, deformed heads, and eyes.

The Measure of Bioaccumulation of GQDs in Zebrafish

First, the standard curves are built. (1) The 1000 mg·L⁻¹ AGQD and CGQD dispersions were diluted in gradient steps to 10 mL, resulting in 12 solutions with concentrations of 0.1, 0.5, 1, 2, 5, and 10 mg·L⁻¹ for both AGQD and CGQD. (2) Take 1 mL of ultrapure water and use the Hitachi F-7000 fluorescence spectrometer (voltage 950 mV, slit width Ex 5 nm, Em 5 nm) to measure the fluorescence intensity of AGQD (Ex 379, Em 480) and CGQD (Ex 395, Em 487) at their respective excitation and emission wavelengths. Repeat the measurement 3 times and calculate the average. (3) Measure the fluorescence intensity of the 12 solution groups at their corresponding excitation and emission wavelengths. Each group is measured 3 times, and the average value was taken. Subtract the fluorescence intensity of ultrapure water from the fluorescence values of each group to obtain the fluorescence standard curve for AGQD and CGQD at the corresponding concentrations. (4) Use the direct proportional relationship $F = kc$, perform a linear regression to fit the standard curve of fluorescence intensity F versus solution concentration c.

The Measure of Bioaccumulation of GQDs in Zebrafish

After 96 hours of exposure, weigh the empty centrifuge tubes. Transfer the larvae from the 24-well plate to 10 mL centrifuge tubes, remove the exposure solution by aspiration, rinse with ultrapure water, and then remove excess water by aspiration. Weigh the tubes again and calculate the average weight of the 15 groups of larvae. After weighing, add 1.5 mL of ultrapure water and a grinding bead to each centrifuge tube. After centrifugation, measure the fluorescence intensity of the supernatant.

The GQD accumulation is determined by measuring the fluorescence intensity of the centrifugation supernatant. (1) Take 1 mL of supernatant from each centrifuge tube and measure the fluorescence intensity at a voltage of 950 mV, slit width Ex 5 nm and Em 5 nm. Repeat the measurement 3 times and calculate the average value. (2) Subtract the average fluorescence intensity of the exposure groups from the blank control group to obtain the fluorescence intensity of the materials at each concentration. (3) Based on the standard curve, calculate the concentrations of AGQDs and CGQDs. (4) Multiply the AGQDs and CGQDs concentrations by the 1.5 mL volume of ultrapure water to calculate the bioaccumulation mass for each group (AG-0.5, AG-5, CG-0.5, CG-5) and the ratio of this bioaccumulation mass to the average weight of the larvae. This gives the proportion of the GQD accumulation mass in the larvae.

Data Analysis

The data of all processing groups were expressed as the average of three independent experiments, and the plots were processed using Excel and Origin.

Results and Discussion

The Observation of Toxicity of AGQDs and CGQDs on Zebrafish

To analyze the effects of two GQDs on the growth and development of zebrafish embryos and larvae, this study investigated the toxicity indexes including mortality, malformation rate, hatchability, autonomic movement frequency and heartbeat frequency within 20 s, and body length during acute exposure of AGQDs and CGQDs to 96 hpf.

Effect of AGQDs and CGQDs on Mortality Rate of Zebrafish

The effect of AGQDs and CGQDs on mortality rate of zebrafish at different exposure times and concentrations is shown in Figure 3.

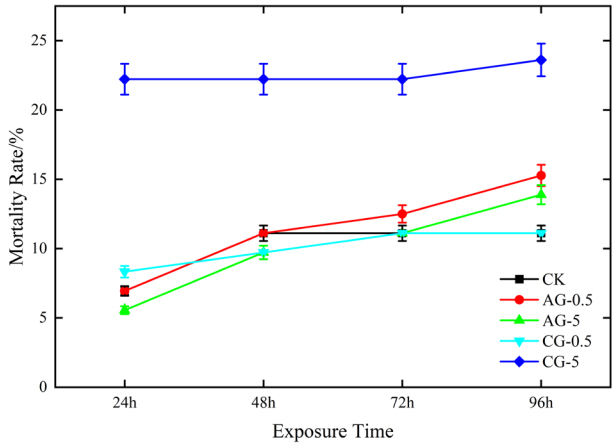

Figure 3. Effects of AGQD and CGQD on mortality rate of zebrafish

As shown in Figure 3, from 24 hpf to 96 hpf, although the mortality rate gradually increased over time in all exposure groups, there were no significant differences between AG-0.5, AG-5, and CG-0.5 compared to the CK (blank control group) ($P > 0.05$). However, the mortality rate in the CG-5 group was significantly higher than in the other four groups, remaining above 20%, while the mortality rates in the other four groups were around 5–15%. Statistical analysis also showed $P < 0.05$, indicating a significant difference from the CK group. These results suggest that exposure to AGQD concentrations ranging from 0 to 5 mg·L^{-1} and lower concentrations of CGQD (0 to 0.5 mg·L^{-1}) did not cause a significant impact on the zebrafish mortality rate over a short period of time. However, for CGQD, increasing the exposure concentration significantly increased the mortality rate in zebrafish.

Effect of AGQDs and CGQDs on Malformation Rate of Zebrafish

The effects of AGQD and CGQD at different concentrations and exposure times on the malformation rate of zebrafish are shown in Figure 4. Examples of normal development and malformation of zebrafish are shown in Figure 5.

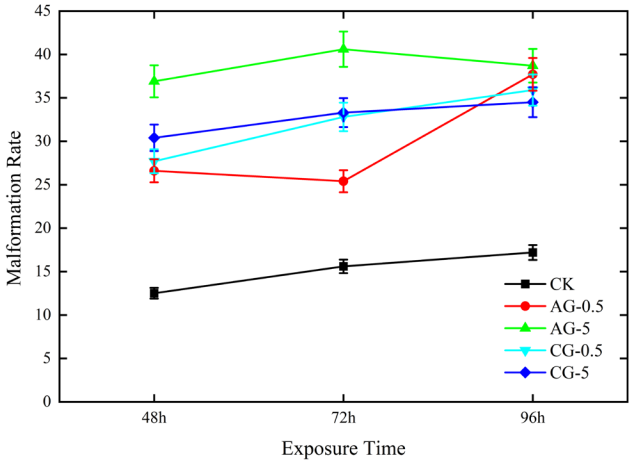

Figure 4. Effects of AGQD and CGQD on malformation rate of zebrafish

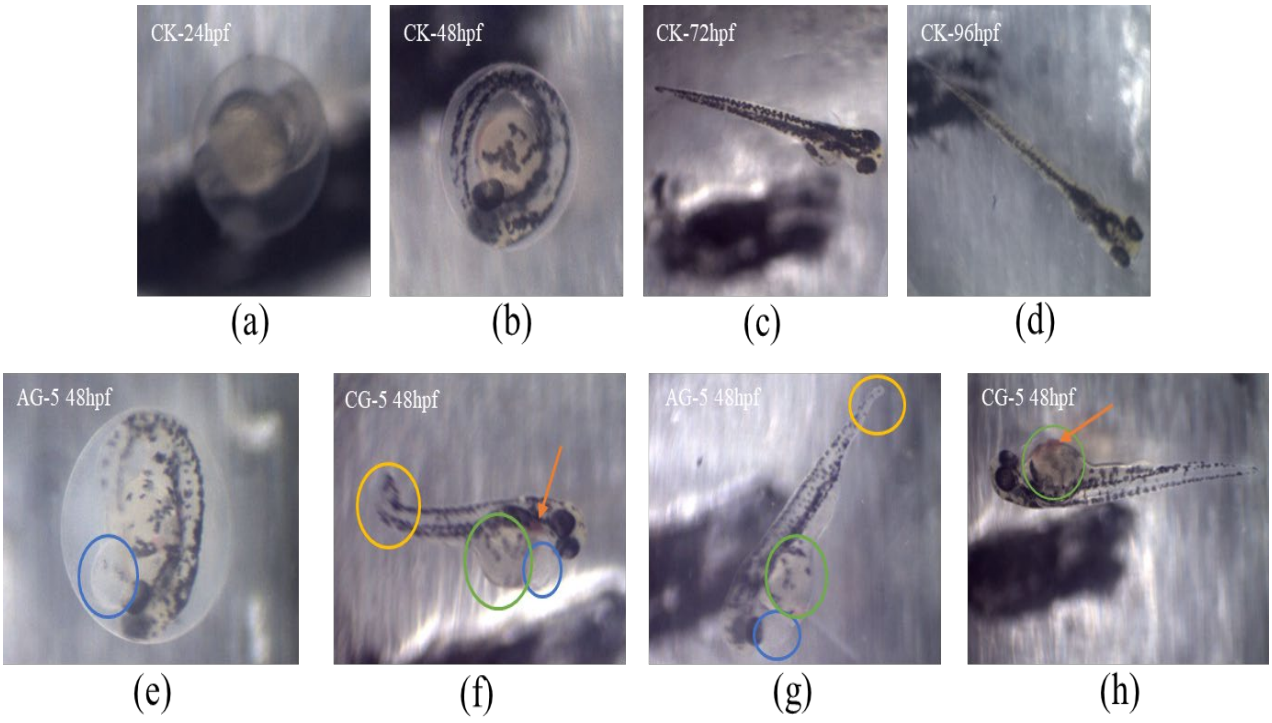

Figure 5. Real examples of normal development and malformation of zebrafish

Note: Normal developmental process of the CK group at 96 hpf (a) (b) (c) (d); Partially malformed zebrafish examples(e) (f) (g) (h), in which the blue circle indicates pericardial edema, the green circle indicates yolk sac edema, the yellow circle indicates a shortened/curved tail, and the orange arrow points to hyperemia of the pericardium and yolk sac.

The malformation rate was calculated as the ratio of the number of malformed individuals to the number of surviving individuals. As shown in Figure 4, the malformation rate in the CK (blank control) group was approximately 15%, while in the experimental groups, the malformation rates were generally above 25%. Statistically, the experimental groups exhibited significant differences compared to the CK group ($P < 0.05$), indicating that even at lower concentrations (0.5 $mg \cdot L^{-1}$), both AGQDs and CGQDs had a pronounced effect on zebrafish developmental malformations. However, no significant differences in malformation rates were observed between the different materials ($P>0.05$). There was no significant difference in malformation rate between groups with different concentrations. The result suggests that even at relatively low exposure concentrations ($c < 0.5$ $mg \cdot L^{-1}$), AGQDs and CGQDs can induce significant developmental malformations in zebrafish embryos and larvae.

Abnormal manifestations include a short or curved tail, edema and hyperemia of the yolk sac and pericardium, deformation of the head and eyes, etc. Edema and hyperemia of the yolk sac and pericardium are common abnormal manifestations, usually caused by abnormal osmotic pressure in vivo, but hyperemia is less common. Since hyperemia is usually caused by abnormal excitability of the vascular constriction and dilation of nerves, the abnormal phenomenon may indicate disruptions in neural activities.

Effect of AGQDs and CGQDs on Hatchability of Zebrafish

The effect of AGQDs and CGQDs on the hatchability of zebrafish at different exposure times and concentrations is shown in Figure 6.

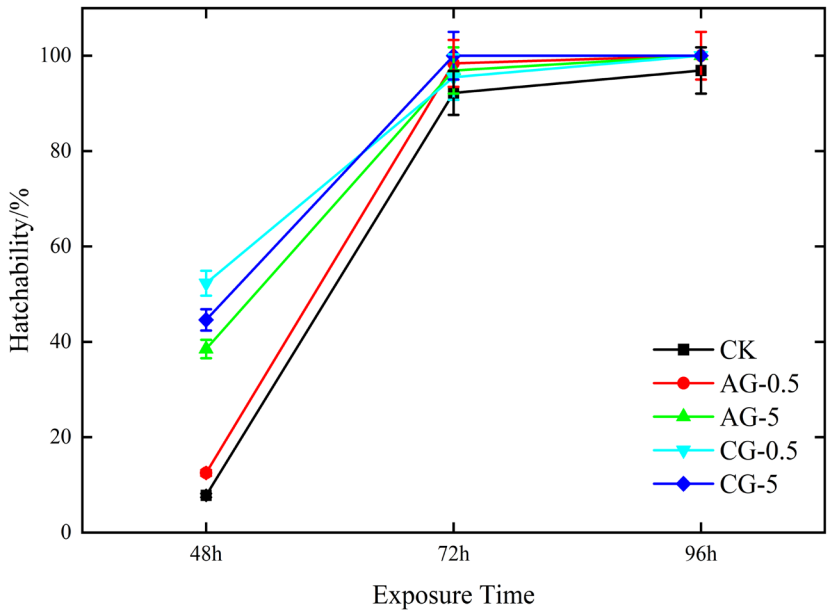

Figure 6. Effects of different concentrations and exposure times of AGQD and CGQD on zebrafish hatch rate

The hatchability was calculated as the ratio of the number of hatched embryos to the number of surviving embryos. In the CK (blank control) group, the hatch rate was approximately 7.8% at 48 hpf, but it increased to 92% at 72 hpf, indicating that most of the zebrafish hatched between 24 hpf and 72 hpf. The hatchability in the AG-5, CG-0.5, and CG-5 groups at 48 hpf was significantly higher than that of the CK group, suggesting that AGQDs and CGQDs exposure stimulated premature hatching in zebrafish embryos. From 72 hpf to 96 hpf, the hatch rates across all groups were similar, and the final hatchability ranged between 95% and 100%. Nearly all zebrafish that survived past 48 hpf had hatched, indicating that exposure to different concentrations of GQDs did not significantly affect hatchability after 48 hpf.

Although some studies have indicated that certain organic pollutants and quantum dots can delay the hatching of zebrafish larvae[31,32], there are also studies suggesting that some pollutants can cause premature hatching of zebrafish embryos at around 48hpf[33,34]. The premature hatching at 24~48 hpf in this study may be due to the toxic property of the exposure material AGQDs and CGQDs, and the lower concentration of exposure. Relevant research points out that the factors leading to embryo hatching mainly include the action of hatching enzymes, embryo twisting, and the peroxidation of membrane lipids[35]. The premature hatching caused by nanomaterials is mainly influenced by peroxidation, where peroxidation products such as Malondialdehyde (MDA) can increase the fragility of cell membranes and destroy cells[36]. In addition, Duc-Hung Pham's research indicates the accumulation amount of silica NPs at chorions is significantly higher than in embryos with 20nm, 50nm, and 80nm silica NPs. Since the particle size of CGQDs and AGQDs is smaller than 10nm, it is speculated that GQDs, not only trigger oxidative stress in zebrafish, producing peroxidation products like MDA, but can also attach to the egg membrane in large amounts, inhibiting and hindering oxygen exchange, further inducing lipid peroxidation of the egg membrane, thereby increasing the fragility of the egg membrane and leading to the premature hatching of zebrafish embryos.

Effect of AGQDs and CGQDs on Spontaneous Movement and Heartbeat of Zebrafish

The effect of AGQDs and CGQDs on spontaneous movement and heartbeat of zebrafish at different exposure times and concentrations is shown in Figure 7.

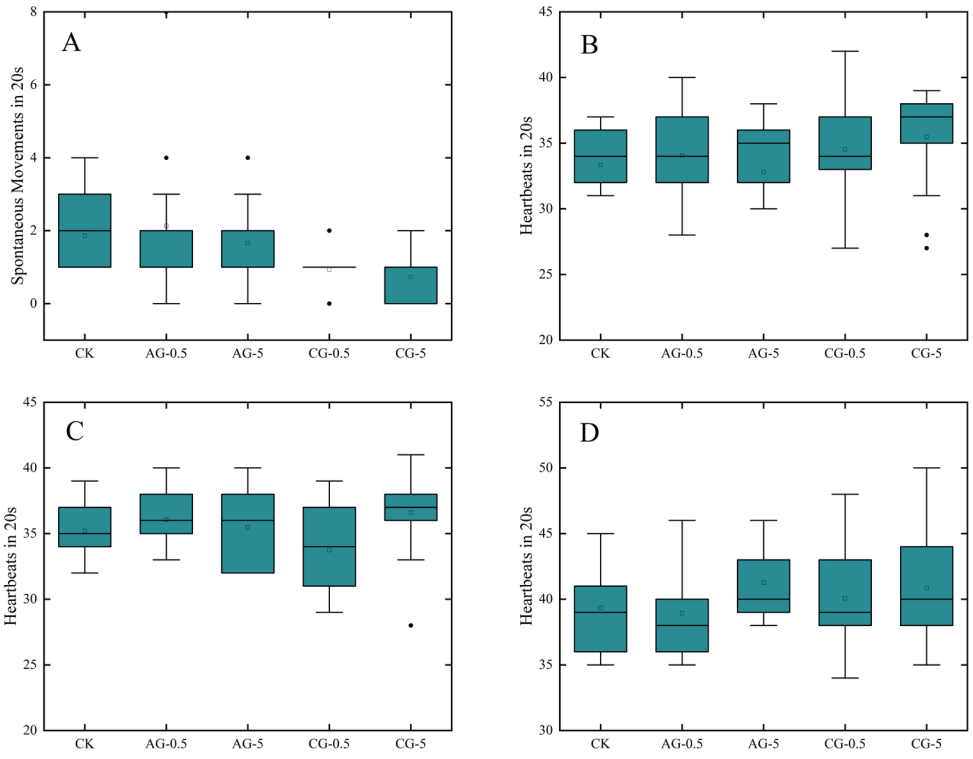

Figure 7. Effects of different concentrations and exposure times of AGQD and CGQD on the spontaneous movements and heartbeat of zebrafish embryos and larvae within 20 seconds.
Note: Spontaneous movements in 20s of randomly selected embryos at A; heartbeat in 20s of randomly selected larvae at B, C, and D.

At 24 hpf, driven by its spinal neurons' network, wild-type zebrafish in embryos spontaneously contract their tail muscles, exhibiting a transient motor movement. A reduction or abnormal alteration in the frequency of these spontaneous movements may indicate dysfunction of the motor nervous system[37,38]. After 24 hours of exposure, 5 samples were randomly selected from each well plate to observe the number of voluntary movements within 20 seconds. After 48 hours of exposure, 5 samples were randomly selected from each well plate to observe the number of heartbeats within 20 seconds.

As shown in Figure 7A, after 24 hours of exposure, the CK group zebrafish embryos exhibited an average of about 2 spontaneous movements within 20 seconds, whereas the CG-0.5 and CG-5 groups showed an average of approximately 1 spontaneous movement within 20 seconds. Compared to the CK group, the early spontaneous movement frequency of zebrafish embryos was significantly reduced under both low and high concentrations of CGQDs exposure ($P < 0.05$). This suggests that CGQDs exposure has a stronger inhibitory effect on vital activities and the nervous system.

As shown in Figure 7 BCD, there were no significant differences in the heart rate of zebrafish between the experimental groups from 48 to 96 hpf. Some groups exhibited slight increases in heart rate, with zebrafish at 96 hpf generally showing faster heart rates. Additionally, after 48 hours of exposure, the heartbeats in the experimental groups were generally more irregular and less rhythmic compared to the CK group.

The repressed spontaneous movements and hyperemia of the yolk sac and pericardium of zebrafish collectively feature the impairment and dysfunction of the nervous system due to AGQDs and CGQDs, in accord with former research on the neurological study of zebrafish. According to a study conducted by Deng[39], significantly weakened baseline motor activity and the appearance of thigmotaxis are signals of disruptive neural behaviors of zebrafish. Moreover, this neural dysfunction occurs at lower concentrations in AGQDs and CGQDs exposure than other nanomaterials. For silica NPs (nanoparticles) exposure[33], only a small percentage of abnormal morphological defects and decreasing spontaneous motor movements is observed at high concentrations (from 12.5 mg·L-1 to 200 mg·L-1); however, in GQDs exposure, only 0.5 mg·L-1 exposure could elicit statistically significant difference on malformation and decreased motor responses and spontaneous movements, indicating a more serious neural injury than other nanoparticle materials. Therefore, the marked decrease in zebrafish's spontaneous propulsive movements and hyperemia at the pericardium and yolk sac together point out that GQDs strongly inhibit nervous system activity, and CGQDs show stronger inhibitory effects than AGQDs.

Effect of AGQDs and CGQDs on Body Length of Zebrafish

The effect of AGQDs and CGQDs on body length at different exposure times and concentrations is shown in Figure 8.

As shown in Figure 8, there was no significant difference in body length among the groups at 96 hpf ($P>0.05$), indicating that the experimental concentrations of AGQDs and CGQDs had no significant impact on the body length development of zebrafish.

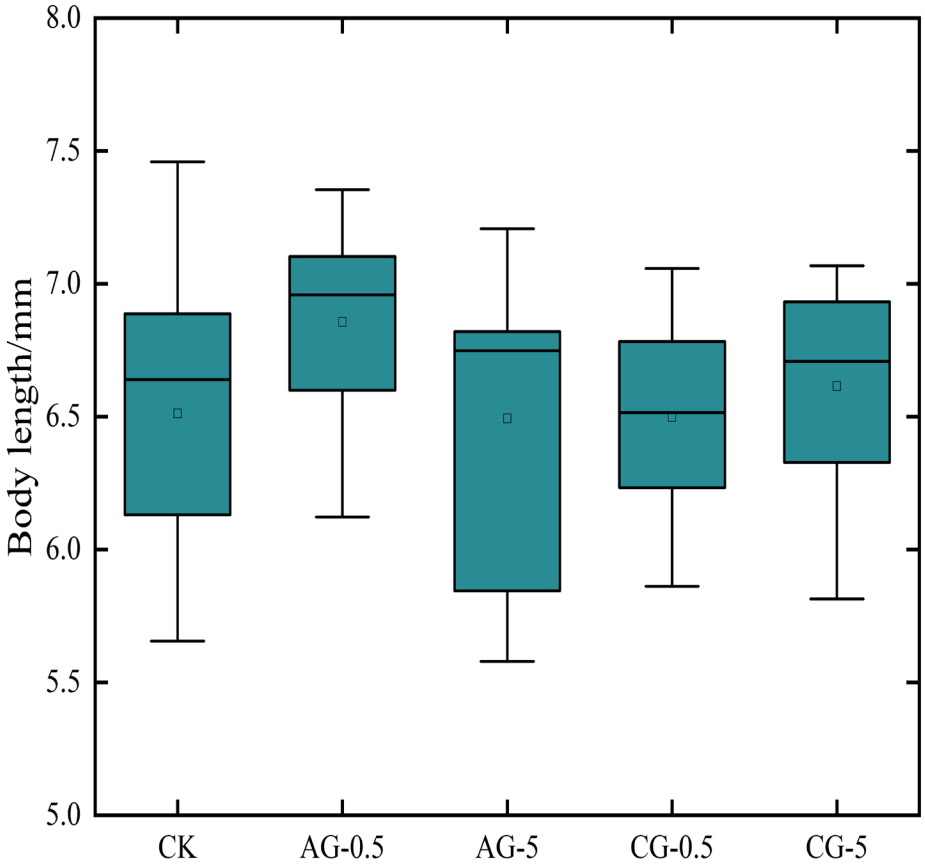

Figure 8. Effects of AGQDs and CGQDs at different concentrations and exposure times on body length of zebrafish larvae

The Measure of Bioaccumulation of AGQDs and CGQDs in Zebrafish

Standard Curve of AGQDs and CGQDs

Take 0.1, 0.5, 1, 2, 5, and 10 mg/L AGQDs and CGQDs solutions, and determine the positive proportional relationship model between the fluorescence intensity (fluorescence value) of the two materials' solutions and the concentration of the substance. Use one-factor linear regression to fit the respective AGQDs and CGQDs fluorescence standard curves. The models were respectively tested using R-squared, multiple R-squared, and adjusted R-squared (Table 2). The fitting curves of the predicted values and measured values in the form of a linear relationship are shown in Figure 9.

Table 2. The linear model of fluorescence intensity and substance concentration of AGQD and CGQD based on spectral parameters

	Excitation, Emission Wavelength/ nm	Linear Regression Model	R Square	Multiple R Square	Adjusted R Square	Standard Error/a.u.
AGQDs	□ 379□ 480□	$Y = 7.64X + 13.19$	0.9139	0.9563	0.8859	11.0170

CGQDs	□ 395□ 487□	$Y = 6.40X - 19.40$	0.9821	0.9921	0.9790	3.7752

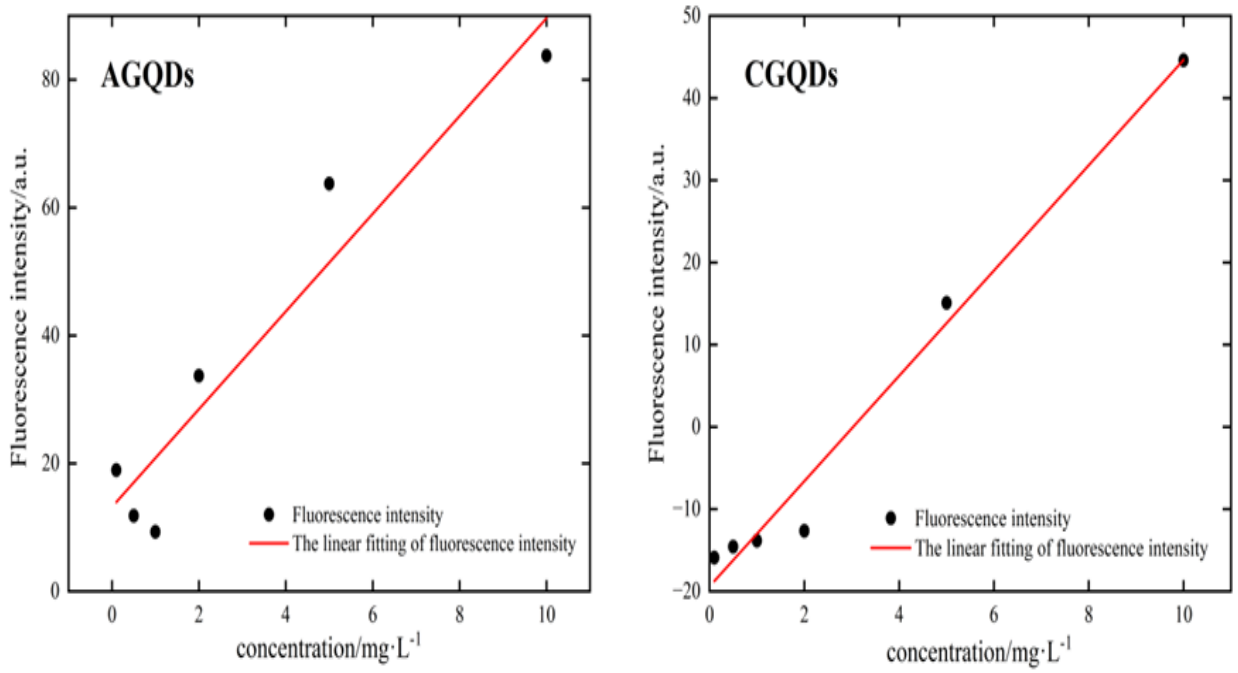

Figure 9. Linear relationship between the measured and predicted fluorescence intensity of AGQDs and CGQDs

Bioaccumulation Amount of AGQDs and CGQDs

Based on the linear regression models of the fluorescence standard curves for AGQDs and CGQDs, as well as the average fluorescence intensities measured for each group, the corresponding GQDs concentrations in zebrafish for each group were determined. The extent of AGQDs and CGQDs accumulation in zebrafish is reflected by the concentration and mass of GQDs in vivo of zebrafish, as well as the accumulative ratio, that is the proportion of GQDs' accumulative mass relative to the total weight of the zebrafish.

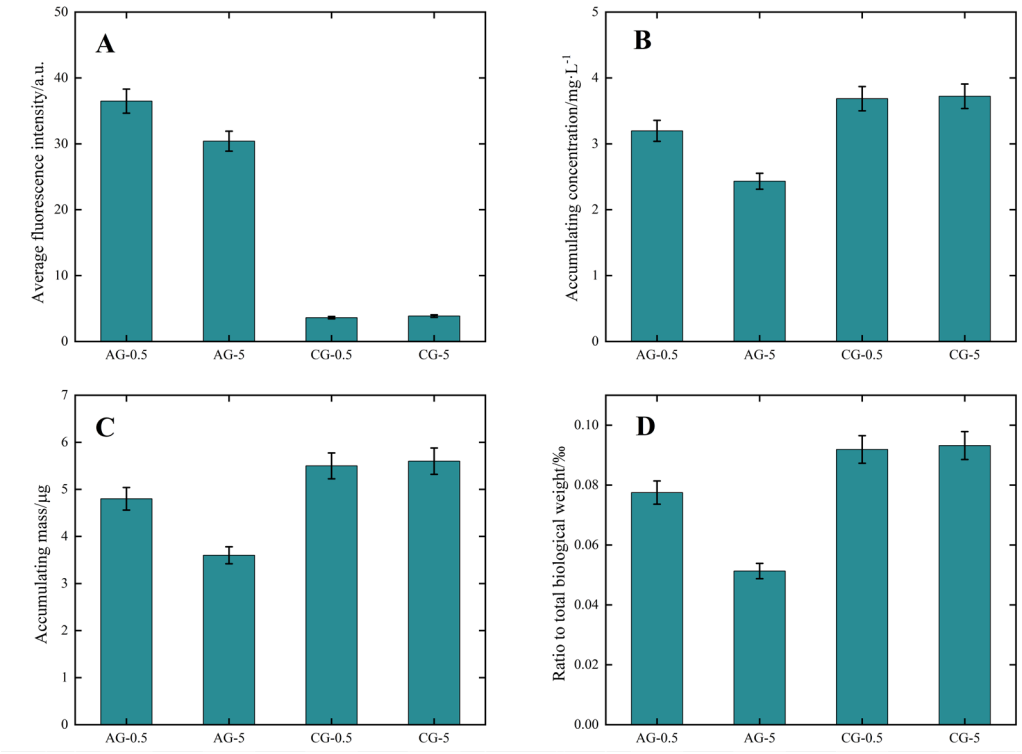

Figure 10. Fluorescence intensity, accumulative concentration, accumulative mass, and accumulative ratio in each group.

As illustrated in Figure 10, the accumulative concentration, mass, and accumulative proportion of GQDs for the groups CG-0.5 and CG-5 both surpass those of AG-0.5 and AG-5. The highest accumulative mass is 5.6 μg in CG-5. No significant disparity in accumulation was observed among groups treated with the same material at varying concentrations. However, the particle size of both types of graphene quantum dots (GQDs) is below 10 nm, with negligible variance, suggesting that particle size exerts a minimal influence on bioaccumulation within the scope of this study. Notably, under identical concentration conditions, CGQDs demonstrate the most pronounced bioaccumulation efficacy.

Our research reveals that CGQDs exert stronger toxicity on zebrafish's early development than AGQDs, according to significantly higher mortality rate, accumulative mass in vivo, and lower frequency of spontaneous movements. Supporting our hypothesis that the toxicity difference between AGQDs and CGQDs at the same concentration is mainly due to its surface carboxyl and amino functional groups, this phenomenon also aligns with the discovery of Sun and Liu[40,41]. Sun's research indicated that GQDs with negatively charged hydroxyl ligands are more active than GQDs with positively charged amine ligands in intracellular peroxidase, superoxide dismutase, and catalase; Liu compared hydroxyl GQDs with amine group compared with carboxyl group GQDs, hydroxyl GQDs resulted in higher ion leakage levels in the root cell membrane. Their finding both suggested that, based on in vitro experiments, GQDs with carboxyl and hydroxyl groups, both containing hydroxyl, cause a more notably destructive impact on cells. In addition, our research, taking advantage of embryos and larvae of zebrafish from in vivo perspectives, corroborates that the toxicity of hydroxyl-functionalized graphene quantum dots is greater than that of carboxyl-functionalized graphene quantum dots, which in turn is greater than that of amino-functionalized graphene quantum dots. Furthermore, toxic destructions caused by carbon nanomaterials like GQDs in cells mainly result from oxidative stress injury, in which the surface of nanomaterials interacts with the cell membrane, generating ROS and disrupting the enzyme's normal function. Thus, it is plausible to contend that high hydrophilicity and high electronegativity y of the carboxyl group

lead to its strong attraction to the cell membrane and more active sites to accelerate peroxidation, which exacerbates cell injury and biological toxicity.

Although some research in the field of biomedicine revealed that functionalized GQDs including AGQDs and CGQDs have high biocompatibility and low toxicity at high concentrations[20,21], our research stresses again its potential developmental toxicity and bioaccumulation in vivo. In many cases, the low cytotoxicity is observed in experiments in vitro (using cells as the model), in low exposure concentrations (lower than 0.5 mg·L-1), in short exposure periods (less than 24hpf), or investigating materials in larger particle size (60-100nm). However, higher concentrations of GQDs due to bioaccumulation and longer exposure periods can enhance toxicity and cell injury. Plus, experiments in vivo reveal more detailed effects such as neural dysfunction and injury that are difficult to detect in vitro experiments, and with smaller particles, GQDs are easier to attach and pass through cell membranes, which induces more destructive effects and oxidative stress. Therefore, our research emphasizes that the toxicity of small particle size nanomaterials like GQDs deserves more research attention to be comprehensively evaluated.

Conclusion

To study the toxicity and bioaccumulation of two surface-modified GQDs, and establish associations between the surface functional modifications and toxicity, we conduct exposure experiments of AGQDs and CGQDs in vivo of zebrafish embryos and larvae. The developmental toxicity of zebrafish by measuring mortality rate, malformation rate, hatchability, frequency of spontaneous movement and heartbeat, and body length; the bioaccumulation is reflected by the concentration and mass of GQDs in zebrafish which are measured by building a fluorescent standard curve of AGQDs and CGQDs. The result indicates that the CGQDs exposure solution at a concentration of 5 $mg{\cdot}L^{-1}$ significantly increased the mortality rate by approximately 100%, showing the strongest toxic effect; a lower exposure concentration (0.5 $mg{\cdot}L^{-1}$) of both AGQDs and CGQDs can induce widespread deformities in multiple organs of zebrafish (pericardial and yolk sac edema, hyperemia, etc.); about 50% of embryos hatch prematurely due to exposure; although there is no significant impact on the speed of heartbeat, the acute exposure to AGQDs and CGQDs weakened the regularity and stability of the zebrafish heartbeat. CGQDs exhibit higher accumulative concentrations, mass, and ratio to the total weight of zebrafish, the accumulative mass being 5.6 μg at both concentrations. The impact of exposure concentration on bioaccumulation appears to be minimal. The differences in toxicity and bioaccumulation between AGQDs and CGQDs are largely related to their surface functional groups: with the hydrophilicity, and electronegativity brought by carboxy and hydroxy, CGQDs may trigger more intense oxidative damage and toxicity.

Still, the experiment has some limitations to be improved in future research. Due to the limited research schedule and resources, we only selected AGQDs and CGQDs as two functionalized GQDs investigated. However, the scale and scope should be expanded to gain a more comprehensive and systematic perspective on the toxic and accumulative effects of GQDs and their surface functional groups. Thus, it is essential to incorporate a wider range of GQDs and other nanomaterials with functional groups in future research.

Based on the above-mentioned toxic properties of AGQD and CGQD, in order to reduce the toxicity of functionalized GQD and its pollution to the ecological environment, chemical modification can be performed to transform them into molecules with lower toxicity and higher biocompatibility. For example, by using its surface activity, hydrophobic functional groups, biocompatible molecules, or environmentally friendly polymers are introduced to its surface through chemical reactions, physical adsorption, electrostatic action, etc., to weaken the cell damage caused by oxidative stress reaction on the surface, or form a protective layer through surface passivation to reduce the exposure of its core high-carbonization and highly toxic structures.

Acknowledgments

The authors sincerely thank Bo Ren and Yuliang Li for their support of the research and paper discussion. The authors also thank the research platform provided by the Talent program.

References

1 Porto, L. S., Silva, D. N., Oliveira, A. E. F. d., Pereira, A. C., & Borges, K. B. (2019). Carbon nanomaterials: synthesis and applications to development of electrochemical sensors in determination of drugs and compounds of clinical interest. *Reviews in analytical chemistry*, *38*(3). https://doi.org/doi:10.1515/revac-2019-0017

2 Lee, J., Mahendra, S., & Alvarez, P. J. J. (2010). Nanomaterials in the Construction Industry: A Review of Their Applications and Environmental Health and Safety Considerations. *ACS Nano*, *4*(7), 3580-3590. https://doi.org/10.1021/nn100866w

3 Yoon, J., Shin, M., Lee, T., & Choi, J. W. (2020). Highly Sensitive Biosensors Based on Biomolecules and Functional Nanomaterials Depending on the Types of Nanomaterials: A Perspective Review. *Materials*(2). https://doi.org/10.3390/ma13020299

4 Maduraiveeran, G., & Jin, W. (2021). Carbon nanomaterials: Synthesis, properties and applications in electrochemical sensors and energy conversion systems. *Materials Science and Engineering: B*, *272*, 115341. https://doi.org/https://doi.org/10.1016/j.mseb.2021.115341

5 Paramasivam, G., Palem, V. V., Meenakshy, S., Suresh, L. K., Gangopadhyay, M., Antherjanam, S., & Sundramoorthy, A. K. (2024). Advances on Carbon Nanomaterials and Their Applications in Medical Diagnosis and Drug Delivery. *Colloids and Surfaces B: Biointerfaces*, *241*. https://doi.org/10.1016/j.colsurfb.2024.114032

6 Cooper, D. R., D'Anjou, B., Ghattamaneni, N., Harack, B., Hilke, M., Horth, A., Majlis, N., Massicotte, M., Vandsburger, L., & Whiteway, E. (2012). Experimental Review of Graphene. *Hindawi*. https://doi.org/10.5402/2012/501686

7 Kurapati, R., Kostarelos, K., Prato, M., & Bianco, A. (2016). Biomedical Uses for 2D Materials Beyond Graphene: Current Advances and Challenges Ahead. *Advanced Materials*, *28*(29). https://doi.org/10.1002/adma.201606523

8 Jastrzbska, A. M., Kurtycz, P., & Olszyna, A. R. (2012). Recent advances in graphene family materials toxicity investigations. *Journal of Nanoparticle Research*, *14*(12), 1320. https://doi.org/10.1007/s11051-012-1320-8

9 Masciangioli, T., & Zhang, W. X. (2003). Peer Reviewed: Environmental Technologies at the Nanoscale. *Environmental Science & Technology*, *37*(5), 102A-108A. https://doi.org/10.1021/es0323998

10 Nel, A., Xia, T., Mädler, L., & Li, N. (2006). Toxic Potential of Materials at the Nanolevel. *Science*, *311*(5761), 622-627. https://doi.org/doi:10.1126/science.1114397

11 Rancan, F., Rosan, S., Boehm, F., Cantrell, A., Brellreich, M., Schoenberger, H., Hirsch, A., & Moussa, F. (2002). Cytotoxicity and photocytotoxicity of a dendritic C(60) mono-adduct and a malonic acid C(60) tris-adduct on Jurkat cells. *Journal of Photochemistry and Photobiology B Biology*, *67*(3), 157-162. https://doi.org/10.1016/S1011-1344(02)00320-2

12 Zakharova, O. V., Mastalygina, E. E., Golokhvast, K. S., & Gusev, A. A. (2021). Graphene Nanoribbons: Prospects of Application in Biomedicine and Toxicity. *Nanomaterials*, *11*(9), 2425. https://doi.org/10.3390/nano11092425

13 Chen, B., Liu, Y., Song, W. M., Hayashi, Y., Ding, X. C., & Li, W. H. (2011). In Vitro Evaluation of Cytotoxicity and Oxidative Stress Induced by Multiwalled Carbon Nanotubes in Murine RAW 264.7 Macrophages and Human A549 Lung Cells. *Biomedical and Environmental Sciences*. https://doi.org/10.3967/0895-3988.2011.06.002

14 Cui, Y., Liu, L., Shi, M., Wang, Y., Meng, X., Chen, Y., Huang, Q., & Liu, C. (2024). A Review of Advances in Graphene Quantum Dots: From Preparation and Modification Methods to Application. *C*, *10*(1), 7. https://doi.org/10.3390/c10010007

15 Chung, S., Revia, R. A., & Zhang, M. (2021). Graphene Quantum Dots and Their Applications in Bioimaging, Biosensing, and Therapy. *John Wiley & Sons, Ltd*(22). https://doi.org/10.1002/adma.201904362

16 Sheikh Mohd Ghazali, S. A. I., Fatimah, I., Zamil, Z. N., Zulkifli, N. N., & Adam, N. A. (2023). Graphene quantum dots: A comprehensive overview. *Open Chemistry*, *21*. https://doi.org/10.1515/chem-2022-0285

17 Kansara, V., Shukla, R., Flora, S., Bahadur, P., & Tiwari, S. (2022). Graphene quantum dots: synthesis, optical properties and navigational applications against cancer. *Materials Today Communications*. https://doi.org/10.1016/j.mtcomm.2022.103359

18 Rosddi, N. N. M., Fen, Y. W., Anas, N. A. A., Omar, N. A. S., Ramdzan, N. S. M., & Daniyal, W. M. E. M. M. (2020). Cationically Modified Nanocrystalline Cellulose/Carboxyl-Functionalized Graphene Quantum Dots Nanocomposite Thin Film: Characterization and Potential Sensing Application. *Crystals*, *10*(10), 875. https://doi.org/10.3390/cryst10100875

19 Lee, B. H., Stokes, G. A., Valimukhametova, A. R., Nguyen, S., Gonzalez-Rodriguez, R., Bhaloo, A., Coffer, J. L., & Naumov, A. V. (2023). Automated Approach to In Vitro Image-Guided Photothermal Therapy with Top-Down and Bottom-Up-Synthesized Graphene Quantum Dots. *Nanomaterials*, *13*. https://doi.org/10.3390/nano13050805

20 Perini, G., Palmieri, V., Ciasca, G., Spirito, M. D., & Papi, M. (2020). Unravelling the Potential of Graphene Quantum Dots in Biomedicine and Neuroscience. *International Journal of Molecular Sciences*, *21*(10). https://doi.org/10.3390/ijms21103712

21 Swidan, M. M., Essa, B. M., & Sakr, T. M. (2023). Pristine/folate-functionalized graphene oxide as two intrinsically radioiodinated nano-theranostics: self/dual in vivo targeting comparative study. *Cancer Nanotechnology*, *14*(1), 1-17. https://doi.org/10.1186/s12645-023-00157-y

22 Wu, K., Zhou, Q., & Ouyang, S. (2021). Direct and Indirect Genotoxicity of Graphene Family Nanomaterials on DNA-A Review. *Nanomaterials (Basel, Switzerland)*, *11*(11). https://doi.org/10.3390/nano11112889

23 Yuan, X., Liu, Z., Guo, Z., Ji, Y., Jin, M., & Wang, X. (2014). Cellular distribution and cytotoxicity of graphene quantum dots with different functional groups. *Nanoscale Research Letters*, *9*(1), 108. https://doi.org/10.1186/1556-276X-9-108

24 Deng, S., Fu, A., Junaid, M., Wang, Y., Yin, Q., Fu, C., Liu, L., Su, D. S., Bian, W. P., & Pei, D. S. (2019). Nitrogen-doped graphene quantum dots (N-GQDs) perturb redox-sensitive system via the selective inhibition of antioxidant enzyme activities in zebrafish. *Biomaterials*, *206*, 61-72. https://doi.org/10.1016/j.biomaterials.2019.03.028

25 Li, M., Gu, M. M., Tian, X., Xiao, B. B., Lu, S., Zhu, W., Yu, L., & Shang, Z. F. (2018). Hydroxylated-graphene quantum dots induce DNA damage and disrupt microtubule structure in human esophageal epithelial cells. *Toxicological Sciences An Official Journal of the Society of Toxicology*(1), 339-352. https://doi.org/10.1093/toxsci/kfy090

26 Liang, L., Shen, X., Zhou, M., Chen, Y., Lu, X., Zhang, L., Wang, W., & Shen, J.-W. (2022). Theoretical Evaluation of Potential Cytotoxicity of Graphene Quantum Dot to Adsorbed DNA. *Materials*, *15*(21), 7435. https://doi.org/10.3390/w13162203

27 Achawi, S., Pourchez, J., Feneon, B., & Forest, V. (2021). Graphene-Based Materials In Vitro Toxicity and Their Structure-Activity Relationships: A Systematic Literature Review. *Chemical research in toxicology*, *34*(9), 2003-2018. https://doi.org/10.1021/acs.chemrestox.1c00243

28 Li, H., Liu, Y., Chen, Q., Jin, L., & Peng, R. (2023). Research Progress of Zebrafish Model in Aquatic Ecotoxicology. *Water*, *15*(9), 1735. https://doi.org/10.3390/w15091735

29 Verma, S. K., Nandi, A., Sinha, A., Patel, P., Jha, E., Mohanty, S., Panda, P. K., Ahuja, R., Mishra, Y. K., & Suar, M. (2021). Zebrafish (Danio rerio) as an ecotoxicological model for Nanomaterial induced toxicity profiling. *Precision Nanomedicine*. https://doi.org/10.33218/001c.21978

30 Westerfield, M. (1995). The zebrafish book : a guide for the laboratory use of zebrafish (Danio rerio).

31 Cahova, J., Blahova, J., Plhalova, L., Svobodova, Z., & Faggio, C. (2021). Do Single-Component and Mixtures Selected Organic UV Filters Induce Embryotoxic Effects in Zebrafish (Danio rerio)? *Water*, *13*(16), 2203. https://doi.org/10.3390/w13162203

32 Kovrižnych, J. A., Sotníková, R., Zeljenková, D., Rollerová, E., & Szabová, E. (2014). Long-term (30 days) toxicity of NiO nanoparticles for adult zebrafish Danio rerio. *Interdisciplinary toxicology*, *7*(1), 23-26. https://doi.org/10.2478/intox-2014-0004

33 Pham, D.-H., De Roo, B., Nguyen, X.-B., Vervaele, M., Kecskés, A., Ny, A., Copmans, D., Vriens, H., Locquet, J.-P., Hoet, P., & de Witte, P. A. M. (2016). Use of Zebrafish Larvae as a Multi-Endpoint

Platform to Characterize the Toxicity Profile of Silica Nanoparticles. *Scientific reports*, *6*(1), 37145. https://doi.org/10.1038/srep37145

34 Maria Violetta, B., & Antonio, S. (2018). Zebrafish or Danio rerio: A New Model in Nanotoxicology Study. In B. Yusuf (Ed.), *Recent Advances in Zebrafish Researches* (pp. Ch. 7). IntechOpen. https://doi.org/10.5772/intechopen.74834

35 King-Heiden, T. C., Wiecinski, P. N., Mangham, A. N., Metz, K. M., Nesbit, D., Pedersen, J. A., Hamers, R. J., Heideman, W., & Peterson, R. E. (2009). Quantum Dot Nanotoxicity Assessment Using the Zebrafish Embryo. *Environmental Science & Technology*, *43*(5), 1605-1611. https://doi.org/10.1021/es801925c

36 Jones, H. B., Garside, D. A., Liu, R., & Roberts, J. C. (1993). The influence of phthalate esters on Leydig cell structure and function in vitro and in vivo. *Experimental and molecular pathology*, *58*(3), 179-193. https://doi.org/10.1006/exmp.1993.1016

37 Saint-Amant, L., & Drapeau, P. (1998). Time course of the development of motor behaviors in the zebrafish embryo. *Journal of neurobiology*, *37*(4), 622-632. https://doi.org/10.1002/(sici)1097-4695(199812)37:4<622::aid-neu10>3.0.co;2-s

38 Sztal, T., Ruparelia, A., Williams, C., & Bryson-Richardson, R. (2016). Using Touch-evoked Response and Locomotion Assays to Assess Muscle Performance and Function in Zebrafish. *Journal of Visualized Experiments*, *2016*. https://doi.org/10.3791/54431

39 Deng, S., Zhang, E., Tao, J., Zhao, Y., Huo, W., Guo, H., Zheng, B., Mu, X., Yuan, K., Deng, X., Shen, H., Rong, H., Ma, Y., & Bian, W. (2023). Graphene quantum dots (GQDs) induce thigmotactic effect in zebrafish larvae via modulating key genes and metabolites related to synaptic plasticity. *Toxicology*, *487*, 153462. https://doi.org/10.1016/j.tox.2023.153462

40 Sun, H., Wang, M., Wang, J., & Wang, W. (2022). Surface charge affects foliar uptake, transport and physiological effects of functionalized graphene quantum dots in plants. *Science of The Total Environment*, *812*, 151506. https://doi.org/https://doi.org/10.1016/j.scitotenv.2021.151506

41 Liu, Z., Li, F., Luo, Y., Li, M., Hu, G., Pu, X., Tang, T., Wen, J., Li, X., & Li, W. (2021). Size Effect of Graphene Quantum Dots on Photoluminescence. *Molecules (Basel, Switzerland)*, *26*(13), 3922. https://doi.org/10.3390/molecules26133922